Proceedings of ICRC 2001: 3939 © Copernicus Gesellschaft 2001

ICRC 2001

3-D anisotropies of galactic cosmic rays: Theoretical modeling

J. Kóta

Lunar and Planetary Laboratory, University of Arizona, Tucson, AZ 85721-0092, USA.

Abstract. We report on 3-dimensional model calculations on the anisotropies of galactic cosmic rays that appear as solar and sidereal daily waves in earth based observations. Both the ecliptic and the sector-dependent North-South components of the anisotropy are considered. Particular attention is paid to the N-S component which is widely used to infer radial gradients and which cannot be properly addressed in 2-D models. We illustrate that the cross-field streaming due to latitudinal gradients may be considerable and the simple picture based solely on the $B \times \nabla U$ streaming may, in some instances, be misleading in inferring the radial gradient. We present 3-D simulations assuming different field models. The concept of upper limiting cutoff rigidity will be addressed. At high rigidities the diffusive description becomes inapplicable. An extension of numerical modeling is proposed for the regime of upper limiting cutoff.

1 Introduction

The transport theory of cosmic rays in the heliosphere (Parker, 1965, 1967; Axford, 1965) is based on the concept of diffusive streaming. The connection between the density gradient, g_j, and the diffusive streaming induced is established by the anisotropic tensor, κ_{ij}, containing three components:

$$\kappa_{ij} = \kappa_{\perp}\delta_{ij} + (\kappa_{\parallel} - \kappa_{\perp})b_i b_j + \kappa_A \, \epsilon_{ijk} \, b_k \tag{1}$$

where b_i is the unit vector pointing along the magnetic field, and ϵ_{ijk} stands for the completely antisymmetric unit tensor.

Inverting the diffusive relation, observed anisotropies may be utilized to infer the gradients, and estimate the diffusion coefficients. The most robust of the anisotropies are the corotational anisotropy lying in the ecliptic plane and the so called $\mathbf{B} \times \nabla U$ anisotropy, i.e. the sector-dependent north-south (N-S) anisotropy ξ_{NS}, normal to the ecliptic plane. ξ_{NS} changes direction as the Earth moves from one polarity sector to the other. The particular significance of ξ_{NS} is that it can be employed to obtain a direct estimate on the radial gradient of galactic cosmic rays (GCR) (Bercovitch, 1970; Swinson, 1971). Ahluwalia (1994) made efforts to determine other components of the gradient from the observed ecliptic anisotropy components, ξ_r and ξ_a. A sophisticated analysis based on all three components of ξ has been carried out by Bieber and Chen (1971). Recently Belov and Oleneva (1997) inferred gradients from the N-S anisotropy.

Theoretical cosmic-ray transport models should explain the anisotropies as well. The ecliptic component has a well established 22-year variation. In the $A > 0$ cycles, when the large scale heliospheric magnetic field (HMF) points outward on the northern hemisphere (i.e. the years of seventies and nineties), the corotational anisotropy shifts from its 18 hr phase to earlier hours (Forbush, 1969; Mori, 1975; Bieber and Chen, 1991; Bieber and Evenson, 1997; Munakata et al., 1997). This can be understood as a natural result of particle drifts and implies a radial gradient that cannot fully balance the outward convection. Numerical models including drift reproduce, at least qualitatively, this feature (Potgieter and Moraal, 1985; Kóta and Jokipii, 1985; Kóta, 1999). The sector-dependent N-S anisotropy, on the other, is an inherently a 3-dimensional phenomenon, connected with the waviness of the tilted heliospheric current sheet (HCS) that cannot be properly addressed in 2-D models (Kóta, 1999).

In the present work, we extend our 3-D code, including a wavy HCS and corotating interaction regions (CIRs) (Kóta and Jokipii, 1991) to calculate anisotropies. We consider the 5-25 GV range, where the relative energy loss of GCR is already small, but the diffusive approximation is still valid. At higher rigidities the diffusive description breaks down. It is not clear how the transition occurs; an ad-hoc upper limiting rigidity is commonly introduced (e.g. Bieber and Chen, 1991). Some aspects of the transition regime has been considered by Erdős and Kóta (1980). In the range of the upper cutoff rigidity, we have to consider a new approach that includes scattering but does not rely on the concept of diffusive streaming and by Kóta (1999).

Correspondence to: J. Kóta (kota@lpl.arizona.edu)

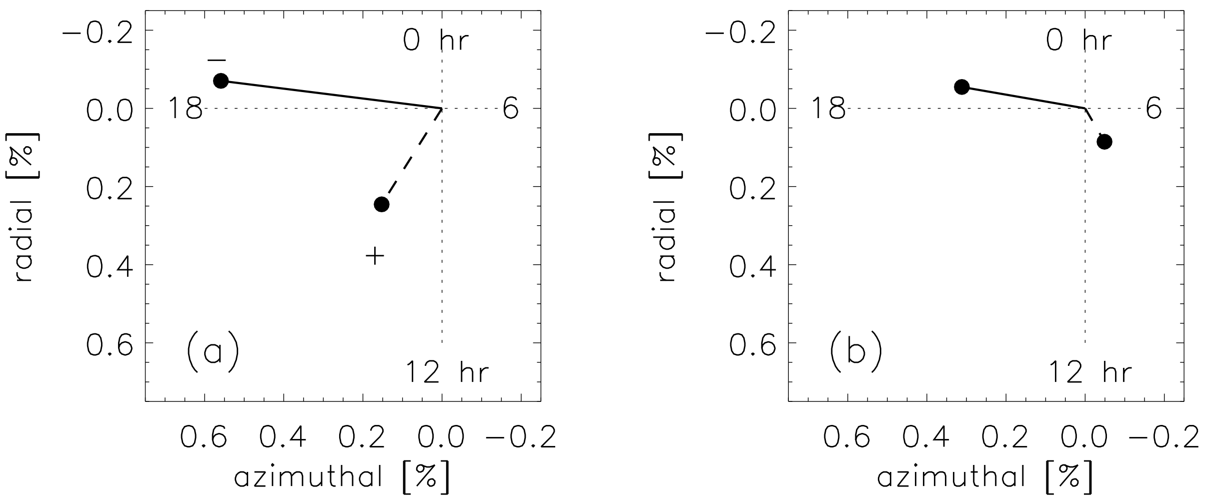

Fig. 1. Harmonic dials for the ecliptic anisotropy components obtained in a 2-D simulation for the two polarity states. The ratios of diffusion coefficients are $\kappa_\| : \kappa_A : \kappa_\perp = 1 : 0.04 : 0.02$ on the left panel (a) and $1 : 0.06 : 0.01$ on the right panel (b). Note the shift toward earlier hours for $A > 0$ (dashed line).

2 2-D Model Simulations

From the point of anisotropies, only the ratios of the diffusion coefficients, $\kappa_\|$, $\kappa_\perp$, and κ_A are important. A uniform increase of all three coefficients would result in proportionally smaller gradients, but anisotropies would remain the same. There are two widely used assumptions based on physical considerations. First, the anti-symmetric component is expected to be $\kappa_A \approx v\rho/3$ where ρ is the particle gyro-radius in the given position in the HMF. Second, a frequently adopted approach is the so-called billiard-ball scattering, assuming that particle motion can be described as regular spiral motion with random and *isotropic* scattering. This leads to the relation (Forman and Gleeson, 1975)

$$(\kappa_\| - \kappa_\perp)\kappa_\perp = {\kappa_A}^2. \tag{2}$$

The billiard ball model deserves special attention. While the term ‘billiard-ball’ might suggest large-angle scattering, the only important assumption is that scattering is isotropic, small angle scattering leads to the same conclusion (Kóta, 1999). It is easy to see that, in a symmetric 2-D model, billiard-ball scattering cannot produce finite azimuthal anisotropy, ξ_a, near the HCS. To obtain co-rotational anisotropy one requires a $\kappa_\perp$ that considerably exceeds the billiard-ball value (Kóta, 1999).

Figure 1 shows the ecliptic anisotropies, ξ_r and ξ_a obtained in a 2-D model, assuming a flat HCS and a uniform 400 km/s solar wind speed, for two sets of parameters. All three coefficients, $\kappa_\|$, $\kappa_\perp$, and κ_A were taken to scale inversely proportional to the magnetic field strength. The left panel shows results obtained with $\kappa_A/\kappa_\| = 0.04$ and $\kappa_\perp = 0.02\kappa_\|$, implying that $\kappa_\perp$ is significantly larger than the value that would be obtained form a billiard-ball scattering. The predicted anisotropies clearly demonstrate the phase-shift to earlier hours in the $A > 0$ cycle. The right panel shows results obtained with $\kappa_A/\kappa_\| = 0.06$ and $\kappa_\perp/\kappa_\| = 0.01$, which are closer to the billiard-ball scattering. The predicted anisotropy decreases for $A < 0$ and almost completely disappears for $A > 0$.

We find that a 2-D model can qualitatively reproduce the observed shift of the ecliptic anisotropy if $Q = \kappa_\|\kappa_\perp/({\kappa_A}^2 + \kappa_\perp^2) \gg 1$. A set of ‘billiard ball ratios’ (Q = 1), would give $\xi_a = 0$ near the HCS, and very little anisotropies away from the HCS.

The N-S anisotropy cannot be properly addressed in a 2-D model; assuming a flat sheet and N-S symmetry does not permit any ξ_{NS} at the current sheet. Moreover, away from the HCS, 2-D models would predict equatorward streaming for $A > 0$, which is contrary to expectations from $\mathbf{B} \times \nabla U$ (Kóta, 1999).

3 3-D Tilted Dipole Model

First we consider a tilted dipole model containing a wavy HCS and a uniform solar wind speed at 400 km/s, i.e. without including CIRs. Figure 2 shows simulation results obtained for 5 GV cosmic rays with parameters similar to those used in our simulation of cosmic-ray transport (Kóta and Jokipii, 1991; 1998). We take $\kappa_A = v\rho/3$, $\kappa_\| = 25\kappa_A$, $\kappa_\perp = 0.02\kappa_\|$, and a tilt ange of 30^o. Our model assumes quasi-steady conditions in the frame co-rotating with the Sun. As the Sun rotates, the Earth’s position changes with respect to the HCS leading to recurrent 27-day variations in the anisotropies and local gradients. Azimuthal gradient produce 27-day intensity waves ($\Delta J/J$ in the lower left panel).

Figure 2 indicates some variability in the anisotropies and spatial gradients during a solar rotation. The spikes at sector-

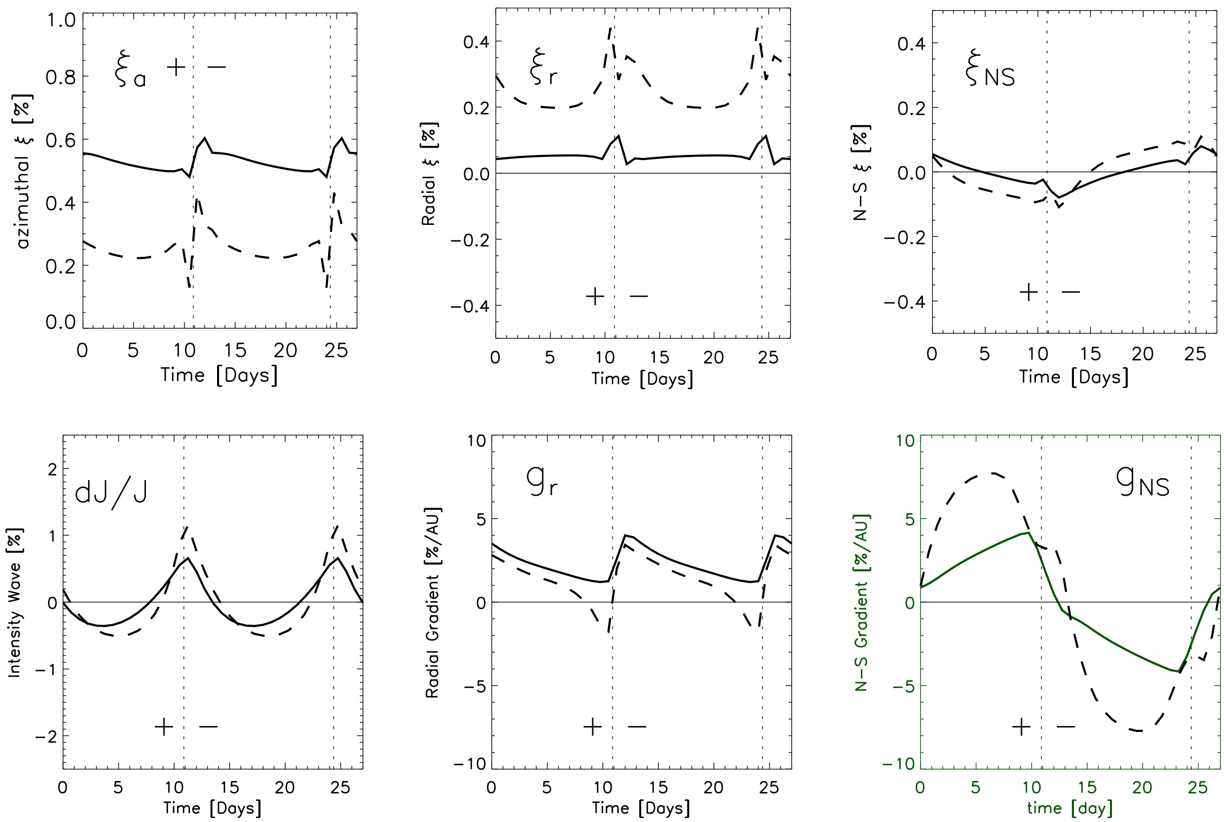

Fig. 2. Anisotropies (upper panels) and gradients (lower panels) at the orbit of Earth as obtained for 5 GeV GCRs in a 3-D simulation with a wavy HCS ($\alpha = 30^o$), but without CIRs, for $A < 0$ (solid lines) and $A > 0$ (dashed lines) in a 27-day rotational period. Vertical dotted lines indicate sector crossing. The lower-left panel shows the predicted recurrent 27-day intensity variations due to azimuthal gradients.

crossing may be artifacts. The ecliptic components show the characteristic phase shift in the $A > 0$ cycle. The radial gradient turns out smaller for $A > 0$. The recurrent 27-day (in fact 13.5 day) variation shows intensity maxima at sector crossing and minima away from the HCS for both polarities.

Latitudinal gradients point northward in the positive and southward in the negative sectors in accord with the direction of the $\mathbf{B} \times \mathbf{V}$ electric field. By contrast with the 2-D simulation, a finite sector dependent ξ_{NS} anisotropy arises. ξ_{NS} does not, however, strictly follow the sectors. For $A > 0$, cross-field diffusion due to the large latitudinal gradient happens not only to balance but even to overcompensate the $\mathbf{B} \times \nabla U$ streaming. For this particular set of parameters, the sector dependent ξ_{NS} could not be reliably used to infer the radial gradient.

4 3-D Quadrupole Model

The tilted dipole model describes the quiet heliosphere. The HCS extends to high latitudes and the quadrupole moments of the field increase as the Sun enters a more active phase. This results in a 4-sector configuration. In this section we report on model simulations with a field resembling that observed at high solar activity.

Figure 3 shows how the predicted ecliptic anisotropies do change when more complex configurations are considered. Panel (a) displays the harmonic dial for the average anisotropies obtained for the tilted dipole model. The phase shifts toward earlier hours for $A > 0$. Panel (b) shows model simulations using the same diffusion coefficients, and uniform solar wind speed as previously, but assuming a 4-sector HMF, by adding a significant quadrupole component to the solar magnetic field. The resulting HCS extends to latitudes as high as 60^o (for details see Kóta and Jokipii, this volume). Inspection of Figure 3 shows that, while the sense of the differences remain similar, the anisotropies predicted for the two different cycles move closer to each other as the HCS becomes more complex.

Panel (c) illustrates the predicted anisotropies when, in addition to the 4-sector quadrupole field, CIRs are also included. The same parameters are used as previously, but the solar wind speed at the Sun is assumed to vary from 350 km/s around the current sheet to 550 km/s at high speed coronal holes. Our code calculates the radial and time evolution of the HCS and CIR structure (Kóta and Jokipii, 1991), which serves then as a background for the transport of GCR. The resulting ecliptic anisotropies remain similar to those obtained without CIRs (panel b), but predictions for the two polarity

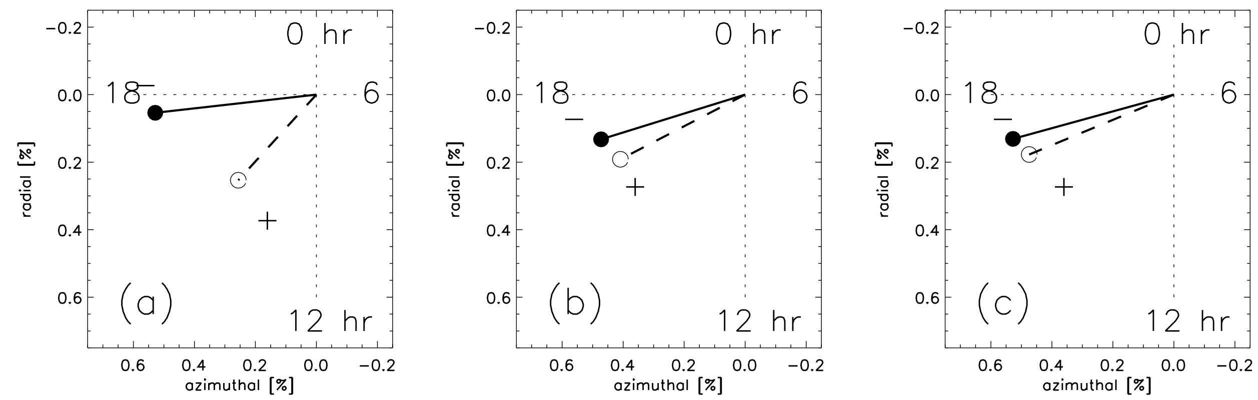

Fig. 3. Ecliptic anisotropy components obtained for $A < 0$ (-) and $A > 0$ (+) cycles for models: (a) tilted dipole model with $\alpha = 30^o$ (b) quadrupole field added (c) quadrupole field plus CIRs added (see text). Note the diminishing phase difference.

states become even closer.

The predicted north-south anisotropy, ξ_{NS}, does also undergoe a remarkable change as we consider more and more complex HMF. In all of our 3-D simulations, ξ_{NS} showed considerable azimuthal variations as the phase of observer changed with respect to the HCS, and also due to azimuthal variation in the solar wind speed and magnetic field (when CIRs were included).

Comparing averages over respective sectors, we found that ξ_{NS} cannot be used to obtain the average radial gradient for the highly organized tilted dipole model. On the other hand, the $\mathbf{B} \times \nabla U$ method becomes better for the less organized 4-sector configuration. We find that the direct application of this method tends to underestimate the radial gradient by a factor of 2 for the 4-sector model without CIRs and it becomes quite accurate (within 10 %) for the quadrupole model including CIRs. The reason is that the sector-averaged latitudinal gradient, which is substantial in the highly organized dipole field (see g_{NS} in the lower right panel of Figure 2) becomes small in the less organized quadrupole field.

5 Conclusions

We have extended our 3-D cosmic-ray transport code to study anisotropies in 2-D and 3-D simulations. We reported on preliminary results in the 5-25 GeV range. Computational refinements are still required and are in progress. The observed phase shift of the ecliptic component is qualitatively reproduced in 2-D and 3-D models for a wide range of parameters. We find that $\kappa_\perp$ needs to be substantially larger than what would be obtained from a ‘billiard-ball’ scattering.

The sector-dependent north-south anisotropy represents a more subtle problem. Our preliminary results suggest that the straightforward application of the standard $\mathbf{B} \times \nabla U$ procedure (Bercovitch, 1970) may be overly simplified and may give inaccurate results for the radial gradient for conditions of the quiet heliosphere (i.e. well organized tilted dipole). The method is applicable if the HMF is less organized. This requires further work.

The diffusive description of cosmic ray transport breaks down in the range of the upper limiting rigidity where heliospheric effects cease. Theoretical modeling of the regime of the upper cutoff requires a new approach that includes scattering, but does not introduce a diffusive streaming. We are developing such a numerical code based on previous theoretical studies (Kóta, 1999). We anticipate to present preliminary results at the Conference.

Acknowledgements. This work has been supported by NASA under grants NAG5 4834 and by NSF under grant ATM 9616547.

References

Ahluwalia, H. S., *J. Geophys. Res., 93*, 23 515, 1994.
Axford, W. I., *Planet. Space Sci., 13*, 115, 1965.
Belov, A. V. and Oleneva, V. A., *Proc. 25th Int. Cosmic Ray Conf., 2*, 157, 1997.
Bercovitch, M., *Acta Phys. Hung., 29 Suppl.*, 169, 1970.
Bieber, J. W. and Chen, J., *Astrophys. J., 372*, 301, 1991.
Bieber, J. W. and Evenson, P., *Proc. 25th Int. Cosmic Ray Conf., 2*, 82, 1997.
Erdős, G. and Kóta, J., *Astrophys. Space Sci., 67*, 45, 1980.
Forbush, S. E., *J. Geophys. Res., 74*, 3451, 1969.
Forman, M. A. and Gleeson, L. J., *Astrophys. Space Sci., 32*, 77, 1975.
Kóta, J., *J. Geophys. Res., 104*, 2499, 1999.
Kóta, J. and Jokipii, J. R., *Proc. 19th Int. Cosmic Ray Conf., 4*, 453, 1985.
Kóta, J. and Jokipii, J. R., *Geophys. Res. Lett., 18*, 1797, 1991.
Kóta, J. and Jokipii, J. R., *Space Sci. Rev, 83*, 137, 1998.
Munakata, K., Miyasaka, H., Hall, D. L., Yasue, S., Kato, C., Fujii, Z., Fujimoto, K., and Sakakibara, S., *Proc. 25th Int. Cosmic Ray Conf., 2*, 77, 1997.
Mori, S., *Proc. 14th Int. Cosmic Ray Conf., 4*, 1209, 1975.
Parker, E. N., *Planet. Space Sci., 13*, 9, 1965.
Parker, E. N., *Planet. Space Sci., 15*, 1723, 1967.
Potgieter, M. S. and Moraal, H., *Astrophys. J., 294*, 425, 1985.
Swinson, D. B., *J. Geophys. Res., 76*, 4217, 1971.